9.3 NONLINEAR PLANETARY-WAVE REFLECTION IN AN ATMOSPHERIC GCM

Christopher C. Walker* and Gudrun Mangusdottir
Department of Earth System Science
University of California, Irvine

1. INTRODUCTION

One way of producing longitudinal asymmetries in the atmosphere is by forcing planetary waves by flow past orography or by flow over quasi-stationary, zonally asymmetric heating. Linear planetary-wave theory appears to work well in explaining longitudinal asymmetries. Linear theory holds that planetary waves are excited in midlatitudes and propagate to low latitudes, where they are absorbed near their critical latitude, the latitude at which the background zonal wind matches the zonal phase speed of the wave (e.g., Killworth and McIntyre 1985). However, observations have shown that intense nonlinear wave breaking can take place in low latitudes (e.g., Waugh and Polvani 2000).

It is not clear how these nonlinear wave breaking regions modify the linear description of the wintertime circulation. There is growing evidence that wave breaking at low latitudes may lead to nonlinear reflection, such that reflected waves propagate out of the wave breaking region into midlatitudes (Brunet and Haynes 1996; Magnusdottir and Haynes 1999; Esler et al. 2000; Magnusdottir and Walker 2000; Walker and Magnusdottir 2002). All of these studies are initial value problems with zonally symmetric initial states. In the 3D studies (Magnusdottir and Haynes 1999; Walker and Magnusdottir 2002) the growth of baroclinic disturbances was inhibited by applying Rayleigh friction on the lowest model levels. Thus the role of baroclinic disturbances was not considered even though they have been found to provide important feedback on low-frequency variability (e.g., Branstator 1992).

Here we summarize our study (Walker and Magnusdottir 2003, hereafter WM03) of nonlinear wave reflection in a state-of-the-art atmospheric GCM. Our only simplifications to the model that we run it in perpetual January mode and we consider an idealized lower boundary. A wave train is excited in midlatitudes by a single Gaussian mountain. We use several different mountain heights and observe the response of the model as the height of the mountain is increased. Consistent with earlier studies in more idealized models, we find strong evidence of nonlinear reflection for large-amplitude forcing.

2. MODEL AND PARAMETERS

We use version 3.10.11 of the National Center for Atmospheric Research's Community Climate Model (CCM3), run at a horizontal resolution of T42, with 18 vertical levels (the experimental setup is discussed in more detail in WM03). The model is run in a perpetual January aquaplanet configuration with zonally symmetric sea surface temperatures (SSTs) that are defined to be consistent with wintertime conditions. Note that although the model is forced with axisymmetric SSTs, atmospheric processes such as transient baroclinic disturbances and tropical convection introduce significant zonal asymmetry in the overlying atmosphere.

Topography is included in the model with a Gaussian "ocean mountain" that has a half-width of 1066 km located at 45°N, 90°W (identically shaped topography is considered in Walker and Magnusdottir 2002; Magnusdottir and Walker 2000; Magnusdottir and Haynes 1999; Brunet and Haynes 1996). We consider several different maximum mountain heights, ranging from 0 to 5000 m, although here we concentrate on results for heights of 500, 2000, 3000, and 4000 m. For each mountain height, the model is run for a total of 4015 days, where each day has the diurnally varying solar radiation associated with 15 January. The model comes to a statistical steady state within 90 days, but the first 180 days are disregarded to insure that the transient effects of spinning up the model are eliminated. This leaves a total of 3835 days for each case.

The model configuration discussed above yields

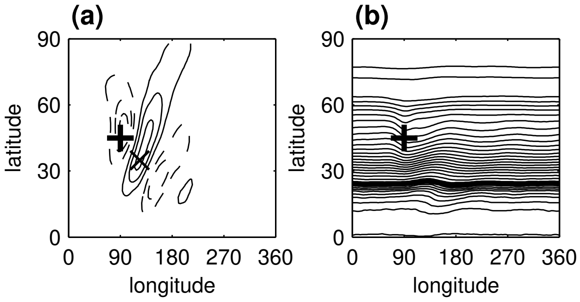

FIG. 1: Mountain height is 500 m. (a) $\overline{v}^{\star}$ (time mean meridional wind with the zonal average removed) on 200 mb surface and (b) time mean PV on 345 °K isentropic surface (corresponds roughly to the 200 mb surface south of 45°N) for 500 m topography. Contour interval in (a) is 1.0 m s^{-1}. Contour interval in (b) is 0.1 PVU (1 PVU = 10^{-6} m^2 s^{-1} K kg^{-1}) from 0 PVU to 1 PVU (south of approximately 25°N), and 0.5 PVU above 1.0 PVU (1 PVU is shown with a thick solid contour). The center of the topography is indicated in both panels with a heavy + symbol. The $\times$ in (a) marks the basis points for the lag correlations shown in Fig. 4

*Corresponding author address: Christopher C. Walker, Division of Geological and Planetary Science, California Institute of Technology, Pasadena, CA 91125 e-mail: chrisw@gps.caltech.edu

zonal and meridional winds that are reasonably close to observed wintertime conditions (see Fig. 1 in WM03). The tropospheric jet is similar in magnitude and location to the observed wintertime jet. Furthermore, as in observations, easterlies are present at all levels in the tropics, guaranteeing that an equatorward propagating quasi-stationary planetary wave train will encounter a critical line. Unlike the real atmosphere, tropical westerlies are not found at any longitudes in the time-mean flow field so that linear propagation across the equator is not possible.

3. RESULTS

Figure 1a shows the time averaged eddy meridional wind, $\overline{v}^{\star}$, on the 200 mb surface for the case forced with the 500 m mountain. The response is broadly similar to earlier work on linear planetary-wave propagation (e.g., Grose and Hoskins 1979), with a wave propagating from the topographical region eastward and toward the equator. This wave is absorbed near its critical line (approximately 10°N at 200 mb) with no sign of reflection.

The time averaged PV field on the 345 K isentropic surface, shown in Fig. 1b, is consistent with indefinite low-latitude absorption. Nonlinear reflection is associated with overturning PV contours caused by breaking waves (e.g., Killworth and McIntyre 1985). In this case, the PV field where the waves impact the critical line (around 15°N, 150°) is only slightly disturbed and does not show signs of wave breaking. Even though the meridional gradient of PV in this area is weak (note that the contour interval in Fig. 1b is 0.1 PVU near the critical line and 0.5 PVU elsewhere) and therefore amenable to overturning, the amplitude of the incident wave train is not large enough to irreversibly mix PV.

As the height of the topography is increased, a wave propagates out of low latitudes toward midlatitudes. This wave train is easily seen in the 3000 and 4000 m cases, shown in Figs. 2b and 2c, respectively, where a wave train originating around 30°N, 180°, propagates northeast into midlatitudes. We believe that this wave train is a result of the nonlinear reflection of the topographically forced planetary wave.

As mentioned earlier, nonlinear reflection is associated with overturning PV contours. In this regard, the PV field for the 4000 m mountain is consistent with reflection out of low latitudes. The time averaged PV field for the 4000 m case, shown in Fig. 2d, is considerably more disturbed where the wave is incident on the critical layer (near 20°N, 150°) than the corresponding PV field for the 500 m case (Fig. 1b). The mean low-latitude PV pattern seen in Fig. 2d is a product of repeated wave breaking. A typical breaking event is seen in Figs. 3a-3f, which show the instantaneous PV field on six consecutive days. Early in this sequence (Figs. 3a and 3b), the PV field does not yet show signs of irreversible mixing. Indeed, there are other instances (not shown) where the PV evolved to a state similar to that shown in Figs. 3a and 3b and then reverted to a more zonal configuration. As the sequence continues, however, it becomes clear that PV is being irreversibly rearranged and the PV field can no longer support linear wave propagation. The wave eventually breaks, such that on the final day of the sequence (Fig. 3f), the ribbon of steep PV gradients no longer shows the overturning, present in Figs. 3c-3e, that characterizes wave breaking. In addition, the PV field shows very small spatial scales, with isolated patches of high-PV air at low latitudes (around 15°N, 170°), in the wave breaking region. It should be noted that the breaking event shown in Figs. 3a-3f is a typical event in a quasi-periodic time sequence.

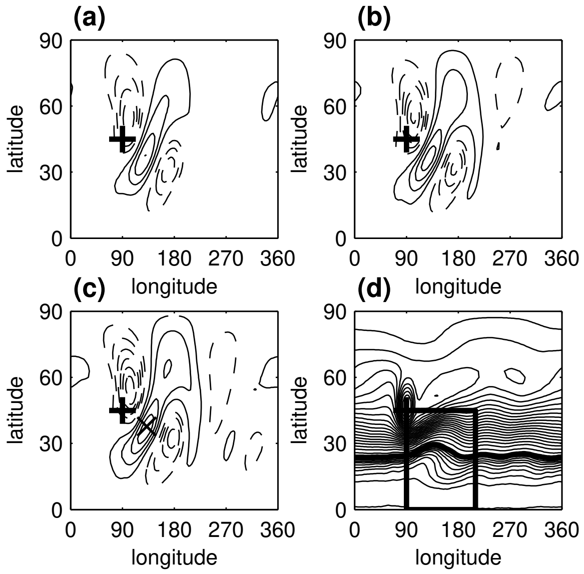

FIG. 2: $\overline{v}^{\star}$ on 200 mb surface for (a) 2000 m topography, (b) 3000 m topography, and (c) 4000 m topography. Panel (d) shows time average PV on 345 °K isentropic surface for 4000 m case. Contour interval in (a)–(c) is 2.0 m s^{-1}. Contour interval in (d) is the same as Fig. 1b. The $\times$ in (c) indicates the basis point for lag correlations shown in Fig. 4. The box in (d) demarcates the region shown in Fig. 3.

Evidence of reflection out of the wave breaking region is corroborated with lagged correlations of the 200 mb eddy meridional wind. We choose as a basis point the location of maximum eddy meridional wind, which is marked on Figs. 1a and 2c with a $\times$ symbol. Lag correlations with this basis point are shown in Fig. 4 for the 500 and 4000 m mountains (see WM03 for lag correlations for additional mountain heights and for lag correlations constructed with an alternate basis point). The long time series (3835 days) leads to high significance; all results shown are significant at the 95% confidence level.

First consider the lag correlations for the 500 m mountain (top row in Fig. 4). In this case, a wave propagates from the topography southeast though the basis point and is dissipated in low latitudes near its critical line. This is contrasted with the 4000 m case, where a wave is clearly seen propagating in an arc out of the wave breaking region (around 30°N, 150°) toward the midlatitudes, turning southward near 45°N, 200°, and impacting low

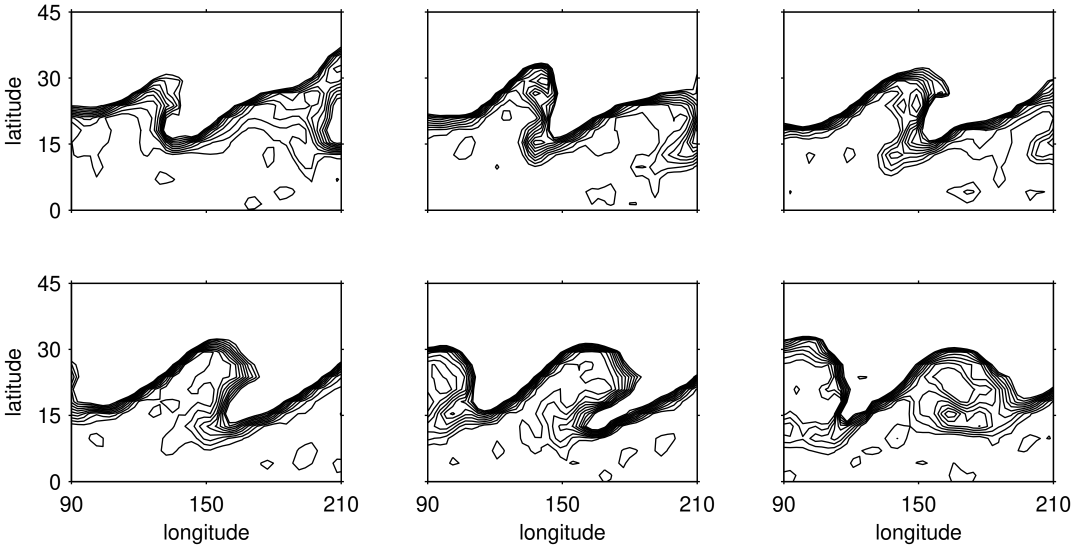

FIG. 3: Instantaneous view of PV on 345 °K isentropic surface for 4000 m mountain. Six consecutive days are shown, starting with panel (a). Only PV from 0.1 PVU to 1.0 PVU is shown, with a contour interval of 0.1 PVU.

latitudes a second time near 20°N, 270°.

The spatial structure of the reflected wave shown in Fig. 4 is very similar to that observed in previous studies. Compare, for example, the wave train in the 4000 m, lag +3 case with the reflected wave in Fig. 10 in Brunet and Haynes (1996), Fig. 15 in Magnusdottir and Haynes (1999), and Fig. 10 in Magnusdottir and Walker (2000). In spite of the different models used in these studies, the signature of the reflected wave is similar in each case. This is to be expected, since the studies all use the same shape topography and consider the wintertime Northern Hemispheric flow. The similarity between our study and the previous studies, however, does lend credence to our claim that nonlinear reflection explains the correlation patterns in Fig. 4.

4. CONCLUDING REMARKS

Using an atmospheric GCM with axisymmetric boundary conditions, we have shown that planetary waves are nonlinearly reflected out of the low-latitude wave breaking region. This is in agreement with a suite of earlier studies in more idealized models (Brunet and Haynes 1996; Magnusdottir and Haynes 1999; Magnusdottir and Walker 2000; Walker and Magnusdottir 2002). We have extended these earlier studies by demonstrating that reflection occurs even in the more realistic setting of an atmospheric GCM. Although the GCM has a simplified lower boundary and is run in perpetual January mode, it is otherwise standard, with all of the processes normally associated with a GCM. Specifically, we have shown that nonlinear reflection exists even in the presence of high-frequency transients, which have been shown to have strong interactions with planetary waves (e.g., Branstator 1992).

Our results are in conflict with those of Cook and

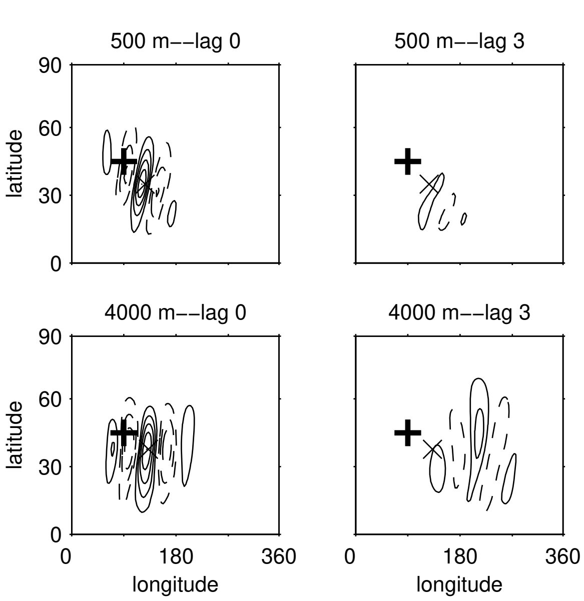

FIG. 4: Eddy meridional wind lag correlations for 500 m case (top row), and 4000 m case (bottom row). Lags considered are 0 days (left column), and +3 days (right column). The $\times$ indicates the basis point and the $+$ indicates the center of topography. Contour interval is 0.2 (zero contour omitted). Dashed contours are negative.

Held (1992, hereafter CH92), who examined the nonlinear response of a simplified GCM to idealized topographical forcing and did not find nonlinear reflection. This motivates the question: why do we see nonlinear reflection while, in very similar experiments, CH92 do not? CH92 pointed out two factors that may have artificially suppressed nonlinear reflection in their experiments and might therefore explain why the two studies arrive at different conclusions. First, CH92 forced their model with annually averaged solar radiation, leading to a very weak Hadley circulation (upper tropospheric meridional wind speed of less than 0.5 m s^{-1}). Studies with simple mechanistic models have indicated that a weak Hadley circulation is associated with a low-latitude flow that does not conserve angular momentum and, consequently, has a steep low-latitude PV gradient (e.g., Fang and Tung 1999). A steep low-latitude PV gradient is resistant to wave breaking and therefore to wave reflection, which depends on PV overturning. CH92 suggested that a stronger Hadley circulation might give a weaker low-latitude PV gradient, leading to increased PV overturning and nonlinear reflection.

To test CH92's idea that the Hadley circulation sets the low-latitude PV gradient and thus exerts a control on nonlinear reflectivity, we conducted experiments (not shown) where our model was forced with the solar radiation of 15 July. The results of these experiments do not support CH92's hypothesis. Although the Hadley circulation is weak (upper tropospheric meridional wind speed of less than 0.5 m s^{-1}), the low-latitude PV gradient in this case is slightly shallower than that of the corresponding 15 January experiments. Accordingly, we find that nonlinear reflection in these experiments is as robust as the reflection shown in section 3.

Although we found that the strength of the Hadley circulation does not explain the discrepancies between our results and those of CH92, the underlying idea — that the discrepancies are due to differences in the low-latitude PV gradient — may still be valid. The zonal wind in CH92's time-average flow is quite different than that in our study. It may be that the low-latitude PV gradient in their case is steeper than in our case. Unfortunately, CH92 do not show their PV profile, so that no comparison can be made.

CH92 also suggest that the coarse horizontal resolution (R15) used in their experiments may have played a role in preventing reflection. To test this hypothesis, we duplicated several of the experiments considered in section 3 at T21 spectral resolution (not shown), where the gridpoint resolution of T21 ($4.5^\circ \times 7.5^\circ$) is similar to that of R15 ($5.6^\circ \times 5.6^\circ$). Although the reflected wave is weaker at T21 than in the equivalent T42 case, reflection still takes place.

Based on our results, we believe that nonlinear planetary-wave reflection plays a role in setting the time averaged wintertime circulation. The wave amplitudes for the 2000, 3000, and 4000 m cases are consistent with the observed stationary wave amplitudes. Furthermore, the model basic state is in accord with the observed zonally averaged Northern Hemisphere wintertime flow. The simplifications made to the model–perpetual January solar radiation and simplified boundary conditions–are made only to isolate and amplify the signal due to reflection. We therefore believe that the model represents the real wintertime atmosphere and that nonlinear reflection is likely occurring in the real atmosphere.

REFERENCES

Branstator, G., 1992: The maintenance of low-frequency, atmospheric anomalies. *J. Atmos. Sci.*, **49**, 1924–1945.

Brunet, G., and P. H. Haynes, 1996: Low-latitude reflection of Rossby wave trains. *J. Atmos. Sci.*, **53**, 482–496.

Cook, K. H., and I. H. Held, 1992: The stationary response to large-scale orography in a general circulation model and a linear model. *J. Atmos. Sci.*, **49**, 525–539.

Esler, J. G., L. M. Polvani, and R. A. Plumb, 2000: The effect of the Hadley circulation on the propagation and reflection of planetary waves in a simple one-layer model. *J. Atmos. Sci.*, **57**, 1536–1556.

Fang, M., and K. K. Tung, 1999: Time-dependent nonlinear Hadley circulation. *J. Atmos. Sci.*, **56**, 1797–1807.

Grose, W. L., and B. J. Hoskins, 1979: On the influence of orography on the large-scale atmospheric flow. *J. Atmos. Sci.*, **36**, 223–234.

Killworth, P. D., and M. E. McIntyre, 1985: Do Rossby-wave critical layers absorb, reflect, or over-reflect? *J. Fluid Mech.*, **161**, 449–492.

Magnusdottir, G., and P. H. Haynes, 1999: Reflection of planetary waves in three-dimensional tropospheric flows. *J. Atmos. Sci.*, **56**, 652–670.

——, and C. Walker, 2000: On the effects of the Hadley circulation and westerly equatorial flow on planetary-wave reflection. *Quart. J. Roy. Meteor. Soc.*, **126**, 2725–2745.

Walker, C. C., and G. Magnusdottir, 2002: Effect of the Hadley circulation on the reflection of planetary waves in three-dimensional tropospheric flows. *J. Atmos. Sci.*, **59**, 2846–2859.

——, and ——, 2003: Nonlinear planetary-wave reflection in an atmospheric GCM. *J. Atmos. Sci.*, **60**, 279–286.

Waugh, D. W., and L. M. Polvani, 2000: Climatology of intrusions into the tropical upper troposphere. *Geophys. Res. Lett.*, **27**, 3857–3860.